FOC based control of a surface-mounted permanent magnet synchronous machine (SPMSM)

Barna Temesi

Abstract—This short design documentation presents the used system model, parameters and control structure that is used for Field-oriented control (FOC) of a SPMSM. The goal of this control system is to achieve maximum-torque per ampere (MTPA).

Index Terms: dynamic modelling of syncronous motors, *dq*-reference frame, PMSM

1 INTRODUCTION

As in every design process, after the problem statement, the system has to be modeled and analyzed. This starts with an overview of the motor parameters. Next, the motor voltage equations, which are already given in the dq-reference frame, are examined. The mechanical equation of the motor is also presented.

2 MODEL OF THE SYSTEM

The motor, in the scope of this thesis, is an SPMSM. This means that the permanent magnets are located on the surface of the rotor. Due to this, the motor is non-salient, and also the reluctance path is equal on the d- and q-axis. This results in equal inductance on the d- and q-axis. For easier understanding, the machine inductance will be denoted as L_s [2].

$$L_d = L_q = L_s \tag{1}$$

The most important parameters of the motor and the other necessary system parameters are listed in the table 1.
As can be seen from the table, the motor has 4 pole pairs. Generally speaking, this means that the machine is more geared towards high-speed operation. In high-torque operation applications, like in the case of a steering motor, the number of poles might exceed a 100.
In simulations, the total system resistance will be used, which takes into account the resistance of every possible component in the setup [1].

Table 1: *System parameters, from previous projects such as*

Description	Notation	Value	Unit
Number of pole pairs	N_{pp}	4	-
Winding resistance	R_w	0.19	Ω
Total system resistance	R_s	0.268	Ω
q and d-axis inductance	L_m	2.2	mH
Rotor PM flux linkage	λ_{mpm}	0.12258	wB
Rated speed, SPMSM	$\omega_{m,rated}$	4500	rpm
Rated torque, SPMSM	$\tau_{m,rated}$	20	Nm
Rated power, SPMSM	$P_{m,rated}$	9.4	kW
Rated speed, IM	$\omega_{IM,rated}$	1400	rpm
Rated torque, IM	$\tau_{IM,rated}$	14	Nm
Rated power, IM	$P_{IM,rated}$	2.2	kW
Rated current, VSI	I_{VSI}	35	A
IM machine inertia	J_{IM}	0.0069	$kg \cdot m^2$
SPMSM machine inertia	J_{SPMSM}	0.0048	$kg \cdot m^2$
Total system inertia	J_{sys}	0.0146	$kg \cdot m^2$
Coulomb friction	C	0.2295	Nm
Viscous friction	B	0.0016655	N

The motor voltage equations are shown in equation (2). Due to the assumption that the system is symmetrical and balanced, the zero term (v_0) is zero.

$$\begin{aligned} v_d &= R_s i_d + p\lambda_d - \omega_r \lambda_q \\ v_q &= R_s i_q + p\lambda_q + \omega_r \lambda_d \\ v_0 &= 0 \end{aligned} \tag{2}$$

In the abc-reference frame, the machine flux-linkage is dependent on position and the machine inductance is constant for a non-salient pole machine, but because the model is already transformed into the $dq0$-reference frame, the machine inductance is constant.

The stator $dq0$-reference frame is aligned with the rotor reference frame, which is naturally in the $dq0$-reference frame. The rotor d-axis is chosen to be aligned with the maximum flux density line at no load condition. The q-axis is always leading the d-axis by 90 degree electric. This way, it is aligned with the minimum flux density line [1].

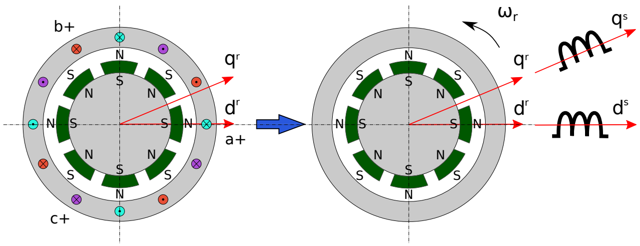

Figure 1: *Reference frame transformation from* ***abc*** *to dq. The structure of the motor is also shown. Inspiration: [3]*

The two d-axis is in line now. This is convenient because, it results in the d-axis and the q-axis flux-linkage as shown in equation (3).

$$\begin{aligned} \lambda_d &= (L_{ls} + L_{md})\, i_d + \lambda_{mpm} = L_d i_d + \lambda_{mpm} \\ \lambda_q &= (L_{ls} + L_{mq}) = L_q i_q \\ \lambda_0 &= 0 \end{aligned} \tag{3}$$

After substitution, the voltage equations may be rewritten as seen in equation (4).

$$\begin{aligned} v_d &= R_s i_d + p(L_d i_d + \lambda_{mpm}) - \omega_r L_q i_q \\ v_q &= R_s i_q + p(L_q i_q) + \omega_r (L_d i_d + \lambda_{mpm}) \end{aligned} \tag{4}$$

Where p is the differential operator $\frac{d}{dt}$. Differentiating the equation, keeping in mind that the derivative of a constant is zero, will result in the following.

$$\begin{aligned} v_d &= R_s i_d + L_d p i_d - \omega_r L_q i_q \\ v_q &= R_s i_q + L_q p i_q + \omega_r (L_d i_d + \lambda_{mpm}) \end{aligned} \tag{5}$$

In one more step, the homogeneous first-order differential equation of the system is acquired.

$$\begin{aligned} \frac{d}{dt} i_d &= -\frac{R_s}{L_d} i_d + \frac{1}{L_d} v_d + \omega_r \frac{L_q}{L_d} i_q \\ \frac{d}{dt} i_q &= -\frac{R_s}{L_q} i_q + \frac{1}{L_q} v_q - \omega_r \frac{L_d}{L_q} i_d - \frac{1}{L_q} \omega_r \lambda_{mpm} \end{aligned} \tag{6}$$

Equations (4) also contain the back-EMF voltage components which are very important in position estimation, hence they are highlighted here:

$$\begin{aligned} e_d &= -\omega_r L_q i_q \\ e_q &= \omega_r (L_d i_d + \lambda_{mpm}) \end{aligned} \tag{7}$$

The governing torque equation can be derived from the equation of the input power of the windings. Simplifying this equation, using the attributions of the SPMSM machine, yields the following expression:

$$T_e = \frac{3}{2} N_{pp} \left(\lambda_d i_q - \lambda_q i_d\right) \tag{8}$$

$$T_e = \frac{3}{2} \frac{N_{poles}}{2} \left(\lambda_{mpm} i_q + (L_d - L_q) i_d i_q\right) \tag{9}$$

$$T_e = \frac{3}{2} N_{pp} \left(\lambda_{mpm} i_q\right) \tag{10}$$

Using Newton's second law, the mechanical equation of the system can be derived as shown in equation (11) [1].

$$T_e = J \frac{d\omega_m}{dt} + B_m \omega_m + T_{dist} \tag{11}$$

Where J is the total system inertia and T_{dist}, the disturbance torque, consists of the load torque and Coulomb friction. The total system inertia includes the inertia of both the IM and PMSM machine and also the coupling and fastening components between them.

The first term is related to the torque needed to accelerate the system without friction, the last two terms are related to the torque which is needed to overcome the viscous friction and the disturbance torque, respectively.

3 Rotor Position Estimation

The goal of this estimator is to estimate the b-EMF voltages in $\alpha\beta$ reference frame and then calculate the rotor position from it. The rotor speed can also be acquired by a simple integration of the rotor position state. The implemented estimator is a sliding mode observer. The theory behind non-linear observer can be found in: [4]. The design is based on [1].

The modified structure of the system, now including the observers, is presented in figure 2.

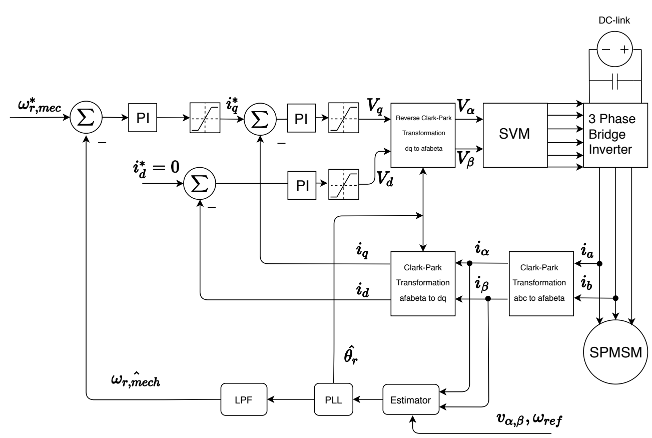

Figure 2: *Structure of control system with a generalized estimator included*

3.1 Sliding mode observer

The sliding mode observer is machine model-based. The starting point of every design is the slightly rewritten voltage equations expressed in the $\alpha\beta$ reference frame.

$$\begin{aligned} \frac{di_\alpha}{dt} &= f i_\alpha + g(v_\alpha - e_\alpha) \\ \frac{di_\beta}{dt} &= f i_\beta + g(v_\beta - e_\beta) \end{aligned} \tag{12}$$

Where $f = -\frac{R_s}{L_s}$ and $g = \frac{1}{L_s}$. The resistance and inductances are time-invariant [1], since with increasing temperature, the resistance increases, and in the meantime, the inductance decreases. However, this effect is assumed to be very minor and will be neglected.

The sliding variable, which characterizes the observer, is chosen as presented in equation (13). Since the system is first-order, the sliding variable directly gives the estimation error.

$$\boldsymbol{\sigma} = (\frac{d}{dt} + \lambda)^{n-1}\tilde{\boldsymbol{x}} = \tilde{\boldsymbol{i_s}} = \hat{\boldsymbol{i_s}} - \boldsymbol{i_s} \tag{13}$$

Where n is the order of the system, $\boldsymbol{\sigma} = [\sigma_\alpha, \sigma_\beta]$, λ is a strictly positive observer variable, and $\tilde{\boldsymbol{x}} = \tilde{\boldsymbol{i}}$ is the error in the estimated stator current [4].

Next, the observer law is formulated, such as [5]:

$$\begin{aligned} \frac{d\hat{i}_\alpha}{dt} &= f\hat{i}_\alpha + g(v_\alpha - ksgn(\sigma_\alpha)) \\ \frac{d\hat{i}_\beta}{dt} &= f\hat{i}_\beta + g(v_\beta - ksgn(\sigma_\beta)) \end{aligned} \tag{14}$$

The main goal is to use the measured states for the calculations and observe the rest of the system equation using the sliding mode observer.
By driving the error between the measured and the estimated currents to zero, the unknown part of the equation (last two terms in equation (14)) is well estimated. This part mainly contains back-EMF terms, and also some unmodelled system dynamics. It is assumed that the back-EMF terms are dominant, therefore the rotor position can be calculated from them with good precision.

The stability of the observer is not discussed here but it can be found in: [1].

The observer gain might be reduced at lower speeds, when the perturbations are also assumed to be less in magnitude. The outcome of it is lower observer activity which reduces the chattering.
Recall that the stability proof defines the following condition. This has to be satisfied all the time.

$$k > max(\mid e_\alpha \mid, \mid e_\beta \mid) \tag{15}$$

The gain may be calculated based on the estimated b-EMF voltages in the previous sampling time *(k-1)*. It can be seen that this not change the stability of the observer, just reduces the stability margin of it.

$$k_k = 100 + \sqrt{e^2_{\alpha,k-1} + e^2_{\beta,k-1}} \tag{16}$$

Where the first term represents a safety, transient term. The measure of it is in voltages.

4 CONCLUSION

For further information please check [1].

REFERENCES

[1] B. Temesi, U. G. Gautadottir, *Sensorless Control of PMSM Drive Using Sliding-Mode-Observers* AAU, Denmark, 2020 Master's thesis.

[2] D. Wilson, *Motor Control Compendium*, 1st-ed . 2011

[3] K. Lu, *Control of Electrical Drive Systems and Converts Lecture 1 Slides*, 1st-ed . pp. 1-30, 2019

[4] J. E. Slotine, W. Li *Applied Nonlinear Control* Englewood Cliffs, New Jersey: Prentice Hall, 1991.

[5] C. Zhou, Z. Zhou, W. Tang, Z. Yu, and X. Sun, *"Improved Sliding-ModeObserver for Position Sensorless Control of PMSM* 2018 Chinese Automation Congress (CAC), 2018, https://ieeexplore.ieee.org/document/8623482/